

CML



Computer Mechanics Laboratory

Technical Report No. 95-023

Nano-Fatigue Wear

by

Z. Jiang, R. Hsiao and D.B. Bogy

Department of Mechanical Engineering
University of California
Berkeley, CA 94720

November 1995

NANO-FATIGUE WEAR

Zhaoguo Jiang, Raymond Hsiao and David B. Bogy

Computer Mechanics Laboratory
Department of Mechanical Engineering
University of California
Berkeley, CA 94720, U.S.A.

A Scanning Probe Microscope (SPM) was used to study nano-fatigue wear. A sharp diamond probe was scanned back and forth over a few micrometers in the same track under controlled micro-Newton loads to determine if fatigue wear occurs when the load is below the critical value that causes single pass wear. Three different results were found, depending on the material. On some materials a few nanometers of wear was noted after a sufficient number of cycles, while in other materials no fatigue wear was detectable. The third, quite unexpected, phenomenon of material build-up, or “negative wear”, was observed on Si. A few hundred cycles produced a few nanometers build-up, the amount being proportional to the load and number of cycles. A raised 2 micron square material build-up patch about 1.5 nm high was formed by repeated raster scanning, and nano-indentation tests were performed which showed that the frictional patch was noticeably harder than the base material. A curve of critical load for nano-fatigue wear initiation versus wear cycles was measured to quantitatively characterize nano-fatigue wear. It is observed the critical load decreases linearly with the logarithm of wear cycle, and there exists an endurance limit. After this endurance limit, the decrease of critical load is not significant. It is concluded that the nano-fatigue wear resistance is closely related with toughness of the materials, since the nano-fatigue wear may be induced by surface or subsurface crack initiation and propagation.

1. Introduction

In a previous study of nano-friction and nano-wear by Jiang et al. (1995a), when a lightly loaded diamond tip was used to scan over various materials with a Friction Force Microscope (FFM), two distinct friction regimes were found: a low friction regime and a high friction regime. For a given tip, the low friction regime occurs at loads below a critical value that is material dependent. In this regime the friction coefficient is independent of material and has the low value of about 0.05. Above the critical load, the friction coefficient increases with load and is material dependent. Furthermore, it was found that the low friction regime was characterized by no wear, i.e., no wear mark could be detected by the scanning probe microscope, whereas a wear mark was always detected in the high friction regime. It was concluded that the no-wear regime was characterized by pure elastic deformation during sliding, while in the wear regime plastic deformation or failure by some other mechanism occurred. The critical load was associated with the yield load of the material based on the maximum Hertzian contact stress. The behavior is similar on layered thin films such as hydrogenated carbon films deposited on silicon substrates (Jiang et al., 1995b) or on magnetic disks (Jiang et al., 1995d) for single-pass sliding nano-friction tests.

The low load and low friction regime, where no wear is observed, has potentially important implications for contact magnetic recording in hard disk drives, a current goal of the disk drive industry, in order to achieve higher data storage densities. If the head-disk system can be designed so that all points of contact in the sliding interface have loads in the low load regime, then a no-wear condition could be expected. Since these

observations were for single pass sliding, and contact recording would have multiple passes over the life time of a drive, the question of fatigue wear due to multiple passes is raised. That is, even if the loads are maintained in the low friction and elastic regime, wear could result from some fatigue failure mechanisms after enough passes. In this research, nano-fatigue wear is investigated for a better understanding of this phenomenon.

2. Experimental Apparatus and Methods

Nano-fatigue wear tests are proposed for investigations of tribological phenomena in the sub-critical load regime (Bogy and Jiang, 1995). A friction force microscope (FFM) with a double parallel-leaf spring tip assembly developed by Lu et al. (1995), which was modified from a FFM by Kaneko et al. (1988), was used to investigate nano-fatigue wear. With this instrument, a sample is attached to a PZT tube scanner by a magnetic force. The PZT tube scanner moves the sample along the X, Y and Z directions with nanometer resolution. A three-sided pyramid diamond tip is mounted on a double parallel-leaf spring unit. A focusing-error detection type optical head is used to measure the vertical deflection of the tip, which determines the normal loading force of the tip. Another optical head of the same type is used to measure the horizontal deflection of the tip, which determines the friction force between the sample and the tip. The resolution of both sensors is better than 1 nm. The SPM is connected through an interface circuit to a controller and uses the control display software of this instrument. Both the surface topography and friction image can be obtained simultaneously. In addition, the friction

signal is directed into a dynamic signal analyzer , so the friction loop can be recorded and processed. The design of the double parallel-leaf spring tip assembly has a special feature that the normal and lateral spring constants can be adjusted independently to meet different test conditions. Moreover, the spring constants are easy to calibrate by use of a layered PZT together with a laser interferometer. All tests were performed in ambient laboratory environment, where the temperature was between 22 ~ 26°C, the humidity was about 34 ~ 41%.

Two **nano-fatigue** wear methods were adopted: raster scanning nano-fatigue wear tests and single-line scanning nano-fatigue wear tests. For raster scanning fatigue wear tests, a diamond tip is controlled to scan over a few micrometers square area on the tested surface with a normal load smaller than the critical load for wear initiation. Then the surface topography of a larger area is measured with the same tip. The wear information can be obtained from the measured image.

For single-line fatigue wear tests, the tip sliding is repeated in the same track on the surface with a normal load smaller than the critical load for wear initiation. Similarly, after the wear tests, the surface is measured and analyzed. The repeated line test is less time-consuming than the raster scanning test, since for the same amount of time during which one wear cycle is completed for the raster scanning test, the number of wear cycles could be 100 ~ 400 with the same scanning speed for the single-line test. However, the raster scanning test may give us more information because of the larger scanned area. It provides a region large enough to analyze by other surface analysis methods.

3. Nano-fatigue Wear on Different Materials

A Mn-Zn ferrite, a hydrogenated carbon film on silicon, a hydrogenated carbon film on a magnetic disk, a @-ion-implanted silicon, a SiO₂ film deposited on silicon, and a silicon wafer were tested by nano-fatigue wear tests using 10,000 wear cycles with a diamond tip with a radius less than 100 nm and a 20 μN normal load. For this tip, the critical loads for wear initiation are between 70 ~ 130 μN for all samples, so the normal load is guaranteed smaller than the critical load for wear initiation. Three distinct results are observed: fatigue wear, no fatigue wear, and frictional material build-up on the sliding track or area, as shown in Fig. 1.

For the @-ion-implanted silicon, no significant change on the tested surface was detectable after the fatigue wear test, which implies that the repeated sliding caused no fatigue wear up to 10,000 wear cycles.

For the Mn-Zn ferrite, the hydrogenated carbon film on silicon, the hydrogenated carbon film on magnetic disk and the SiO₂ film deposited on silicon, observable wear occurred after the tests. The wear depths were from 1 ~ 4 nm. Figure 2 shows a typical single-line wear mark on the carbon film on the silicon substrate after 10,000 wear cycles. The wear depth is 3.8 nm. Roughly, an atomic layer was removed with 300 wear cycles.

A quite unexpected phenomenon was observed on the silicon sample, the interaction contact area on the surface was raised rather than depressed after the tests, or “negative wear” occurred. Figure 3 shows a typical single-line negative wear on the silicon after 10,000 repeated sliding cycles in the same track. The projected height or the

negative wear is about 6.8 nm. Further results and detailed analysis are illustrated in the next sections.

Friction coefficients were also measured during the fatigue wear tests. The value for the friction coefficient remained almost constant from 0.03 ~ 0.06 for all tested samples through 10,000 wear cycles.

4. Frictional Material Build-up on Si

As shown in Fig. 3, an unexpected single-line material build-up was produced when a diamond tip slid repeatedly in the same track with a normal load less than the critical load for wear initiation. Further studies showed that a material build-up also occurred when the tip raster scanned the Si surface. Figure 4 illustrates a typical raster scanned material build-up. After 2,000 raster scans with 20 μN normal load, the whole scratched square area ($2.5 \mu\text{m} \times 2.5 \mu\text{m}$) was raised by 1.5 nm as a patch. --

The build-up is not simply a mechanical relaxation caused by the tip scratch, because the negative wear can be superimposed. Figure 5 shows two overlapped frictional patches on the silicon after 2,000 repeated sliding for each. Obviously, the 2.4 nm height of the overlapped part is the sum of the two patches, which are about 1.2 nm high for each. Based on this phenomenon, a letter "H" could be produced by scratching three single lines on a square build-up patch. Figure 6 shows one of the typical results. A 1 nm high frictional patch of $2.5 \mu\text{m} \times 2.5 \mu\text{m}$ was built first by repeated raster scans. Then a

build-up with a letter "H" shape as high as 1.4 nm was superimposed on the friction patch by repeated line scans on three tracks arranged as "H".

Furthermore, the height of the build-up changes with normal load and number of scan cycles. As shown in Fig. 7, when the number of wear cycles is fixed, which is 5,000 in this case, the build-up height increases with normal load. The relation between them is strongly linear. Hence, a larger normal load remarkably enhanced the driving force for the build-up formation. Figure 8 shows that when the normal load is fixed (which is 20, and 70 μN , in this case), the build-up height increases with wear cycles almost linearly at the beginning. After some wear cycles, say 4,000 for 20 μN and 6,000 for 70 μN , the negative wear does not vary significantly with the wear cycles any more. The sliding thereafter is a no-wear sliding over the built-up surface.

Our results show that the build-up is not sensitive to the scan speed in the tested range, as shown in Fig. 9. In both load cases (100 and 70 μN), the build-up does not change noticeably when scan speed varies from 10 ~ 70 $\mu\text{m}/\text{sec}$.

The mechanical properties were altered on the frictional build-up. Nano-indentation hardness tests using a Scanning Probe Microscopy (Lu et al., 1994) were employed to compare the mechanical properties of the frictional layer with those of the virgin surface. In this test, triangular pyramid diamond tips with tip radii less than 100 nm, which are attached on leaf springs of various lengths for providing different stiffnesses, are controlled by a SPM to conduct both indentation and surface measurement. Indentation is performed by either moving the sample or the tip toward the other. The loading force acting on the tip is calculated by multiplying the tip displacement by the spring constant.

After making the indentation, the surface image is acquired using the same tip scanning the surface, and the indentation mark is measured. The hardness is defined as the ratio of the indentation force to the projected area of the residual indentation. Due to the sub-nanometer resolution of the instrument, hardness tests can be conducted with indentation depths in a range of 1 ~ 100 nm. Indentation depths as small as 1 nm can be made and reliably measured. In addition to the characteristics of high resolution and small indentation depths, the technique has a special advantage of precisely locating the diamond tip at the desired position on the tested surface. For example, it is possible to indent and measure the hardnesses of different single grains no larger than fractions of a micron.

A 1.5 nm high raised frictional material build-up patch of about $2\ \mu\text{m} \times 2\ \mu\text{m}$ was produced on a Si surface. Then nano-indentations were made on both the raised frictional patch and the un-scratched surface by the same tip with the same indentation force, and the hardnesses were obtained. The indentation force was chosen in such a way that the indentation depth was large enough to be measured but not large enough to penetrate through the frictional build-up layer. In this case, the normal load was 300 μN . Figure 10 shows the image of the frictional patch and two indentation marks, one is on the patch, the other is on the virgin surface. The indentation depth on the patch is about 0.8 nm, which is less than the 1.5 nm height of the patch. However, the indentation on the virgin surface is about 1.7 nm, larger than that on the patch. The difference of the indentation sizes indicates that the frictional layer was noticeably harder than the base material. In fact, the frictional layer is about 1.5 times harder than the virgin surface with a hardness

of about 11 GPa. The hardening of the frictional build-up also strongly suggests that the build-up is not a mechanical relaxation.

Kaneko and Hamada (1993) reported that projections were observed on a poly-carbonate, a poly-methyl-meta-acrylate and an epoxy by diamond tip scanning-scratching. However, the loads they used were in a range large enough to cause plastic deformations on the tested surfaces. The projections occurred immediately after the first few wear cycles (1 ~ 11 wear cycles), then peak-and-valleys and ridges (unevenness) were formed, and the scanned surfaces were worn down finally after more wear cycles. Therefore, the projections they observed may be mainly due to mechanical relaxations and plastic distortions of the surface materials. In contrast to their cases, the build-up on Si reported here occurred after several-hundred wear cycles and kept growing up to tens of thousands wear cycles, with a load too small to cause plastic deformations. It is a novel phenomenon which has not been observed on other surfaces.

The possible reasons for the material build-up may be either chemical or physical. For example, oxidization of silicon with oxygen in the air, which is chemical, may occur due to the repeated scans and add more material on the tested surface. It may also happen that the repeated scans change the silicon crystal structure under the scratched area and produce a volume increase. Whatever it is, the phenomenon indicates that not only wear but also negative wear should be well controlled in the head-disk interface of the future contact or near-contact recording, since negative wear will substantially increase the spacing between the slider and the disk and degrade the read-write signal.

5. Critical Load for Nano-fatigue Wear Initiation

In order to quantitatively characterize nano-fatigue wear, a curve of critical load for nano-fatigue wear initiation versus wear cycles was proposed. As described by Jiang et al. (1995a), there is a critical load for wear initiation when a diamond tip scratches over a sample surface for a single-pass. Similarly, there is also a critical load for wear initiation when the tip scans over the sample surface for a certain number of multiple passes or multiple wear cycles.

Figure 11 shows a typical curve of critical load for fatigue-wear initiation versus wear cycles obtained with a diamond tip sliding on a carbon film containing 40 percent hydrogen. It is observed that the critical load decreases rapidly with the wear cycles. The tendency slows down after 100 wear cycles. Figure 12 shows the same plot with the X-axis converted to the logarithm of wear cycles. The critical load for wear decreases linearly with the logarithm of wear cycles at the beginning, then almost levels off after 100 wear cycles.

Figure 13 shows the two curves of critical load for nano-fatigue wear initiation versus wear cycles for two carbon films containing 0 percent and 40 percent hydrogen. The two curves intersect and cross each other, which means that even though the film with 40% hydrogen is softer than the film with 0% hydrogen (the critical load for wear at the single pass of the former is smaller than that of the latter), the nano-fatigue performance of the former is better than the latter. In other words, the harder material, or the material with a better abrasive wear resistance, does not have a better nano-fatigue wear resistance.

The reason is that the wear mechanisms are different. For wear at a single **pass**, the material is in the plastic deformation or plastic flow regime. In this regime, the tip **plows** or cuts the sample surface as shown in Fig. 14. In this case, the harder material has the better wear resistance. Hardness is usually a proper parameter to characterize materials in this regime, since the hardness reflects the ability of the materials against local plastic deformation.

However, the fatigue wear sliding is in the elastic deformation regime. When the tip **slides** over the sample surface, no wear track is detectable. It is hypothesized that tiny cracks are initiated at the surface or under the subsurface layer, as shown in Fig. 15 [(a) and (d)]. These cracks would propagate under multiple passes. After a certain number of wear cycles, these cracks would coalesce with each other, forming chips that drop out. The nano-fatigue wear track is thus formed. Therefore, the nano-fatigue wear resistance is closely related with the fracture toughness of the materials, an ability of materials against crack initiation and propagation. Since a harder material may not have a larger **toughness**, the harder material may not have a better fatigue wear resistance.

Crack initiation and propagation is very sensitive to applied stresses, so the critical load decreases rapidly with wear cycles. However, when the stress reaches a threshold value, the speed of propagation slows down, and a leveling-off occurs in the **curve** of critical load versus wear cycles. The curve of critical load versus wear cycles provides a practical tool for no-wear tribo sliding systems, that is, the normal load on every contact asperity should be smaller than this threshold critical value.

6. Summary and Conclusion

Nano-fatigue wear tests were performed using a scanning probe microscope on several samples such as Si, Mn-Zn ferrite, hydrogenated carbon films on silicon, hydrogenated carbon films on magnetic disks, C⁺-ion-implanted silicon, and SiO₂ films deposited on silicon. No fatigue wear was detectable on the C⁺-ion-implanted silicon after 10,000 wear cycles with a 20 μN load. With the same test conditions, 1 ~ 4 nm deep fatigue wear occurred on the Mn-Zn ferrite, the hydrogenated carbon film on silicon, the hydrogenated carbon film on a magnetic disk, and the SiO₂ film deposited on silicon. “Negative wear”, i.e., a frictional material build-up, was formed on the Si with a load from 15 to 100 μN and wear cycles from 500 to 10,000.

A curve of critical load for nano-fatigue wear initiation versus wear cycles was measured to quantitatively characterize nano-fatigue wear. It is observed that the critical load decreases linearly with the logarithm of wear cycles, and there exists an endurance limit. After this endurance limit, the decrease of critical load is not significant. It is concluded that the nano-fatigue wear resistance is closely related with toughness of materials, since the nano-fatigue wear may be induced by surface or subsurface crack initiation and propagation.

List of Figures

- Fig. 1 Three results from the nano-fatigue wear tests.
- (a) Wear
- (b) Zero-wear
- (c) Negative wear
- Fig. 2 A surface image and section profile of a carbon film on silicon substrate
- Fig. 3 A surface image and section profile of a Si sample
- Fig. 4 A surface image and section profile of a material build-up on a Si
- Fig. 5 A surface image and section profile of two overlapped
frictional material build-up patches
- Fig. 6 A surface image and section profile of a material build-up with a letter “H”
shape superimposed on a frictional build-up patch
- Fig. 7 A plot of material build-up versus normal load
- Fig. 8 A plot of material build-up versus wear cycles
- Fig. 9 A plot of material build-up versus scan speed
- Fig. 10 A surface image and section profile of the nano-indentation marks on both
the build-up and the virgin surface of Si
- Fig. 11 Critical load for nano-fatigue wear initiation versus wear cycles
- Fig. 12 Critical load for nano-fatigue wear initiation versus logarithm
of wear cycles
- Fig. 13 Curves of critical load for nano-fatigue wear initiation versus wear cycles
for two carbon films

Fig. 14 Plastic deformation induced by a diamond tip scratch

Fig. 15 Cracks induced by a diamond tip scratch during a nano-fatigue wear test

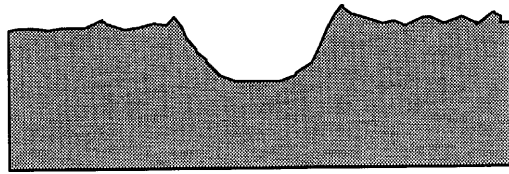
(a) Before the scratch

(b) After the scratch

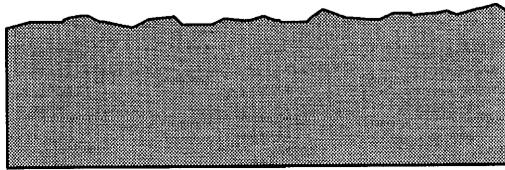
References

- [1] Bogy, D. B., and Jiang, Z., 1995, "Nano-hardness, nano-friction and nano-wear of ultra-thin overcoats", *MRS Symp. Proc., Thin Films: Stresses and Mechanical Properties (V)*, Vol. 356, pp. 737-748.
- [2] Jiang, Z., Lu, C.-J., Bogy, D. B., and Miyamoto, T., 1995a, "Dependence of nano-friction and nano-wear on loading force for sharp diamond tips sliding on Si, Mn-Zn ferrite and Au", *ASME Journal of Tribology*, Vol. 117, No.2, pp. 328-333.
- [3] Jiang, Z., Lu, C.-J., Bogy, D. B., Bhatia, C. S., and Miyamoto, T., 1995b, "Nanotribological characterization of hydrogenated carbon films by scanning probe microscopy", *Thin Solid Films*, Vol. 258, pp. 75-81.
- [4] Jiang, Z., Lu, C.-J., Bogy, D. B., Bhatia, C. S., and Miyamoto, T., 1995d, "Nanotribological evaluations of hydrogenated carbon films as thin as 5nm on magnetic disks", *IEEE Transactions on Magnetics*, Vol. 31, No. 6, pp. 3015-3017.
- [5] Kaneko, R., and Hamada, E., 1993, "Microwear processes of polymer surfaces", *Wear*, Vol. 162-164, pp. 370-377.
- [6] Kaneko, R., Nonaka, N., and Yasuda, K., 1988, "Summery abstract: Scanning Tunneling Microscope and Atomic Force Microscope for Microtribology", *J. Vac. Sci. Technol. A*, Vol. 6, No. 2, pp. 291-292
- [7] Lu, C.-J., Bogy, D. B., and Kaneko, R., 1994b, "Nanoindentation hardness tests using a Point Contact Microscope", *ASME J. of Tribology*, Vol. 116, pp. 175-180.

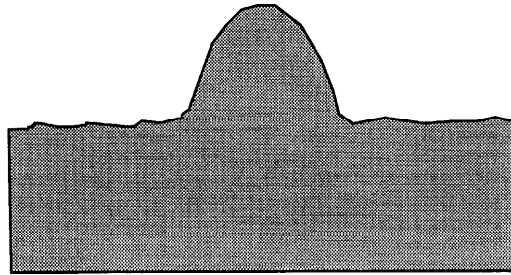
- [8] **Lu, C.-J., Jiang, Z., Bogy, D. B., and Miyamoto, T., 1995a**, “Development of a new tip assembly for lateral force microscopy and its application to thin film magnetic media”, *ASME Journal of Tribology*, Vol. 117, No. 2, pp. 244-249.



(a)



(b)



(c)

Figure 1 Three results from the nano-fatigue wear tests.

(a) Wear

(b) Zero-wear

(c) Negative wear

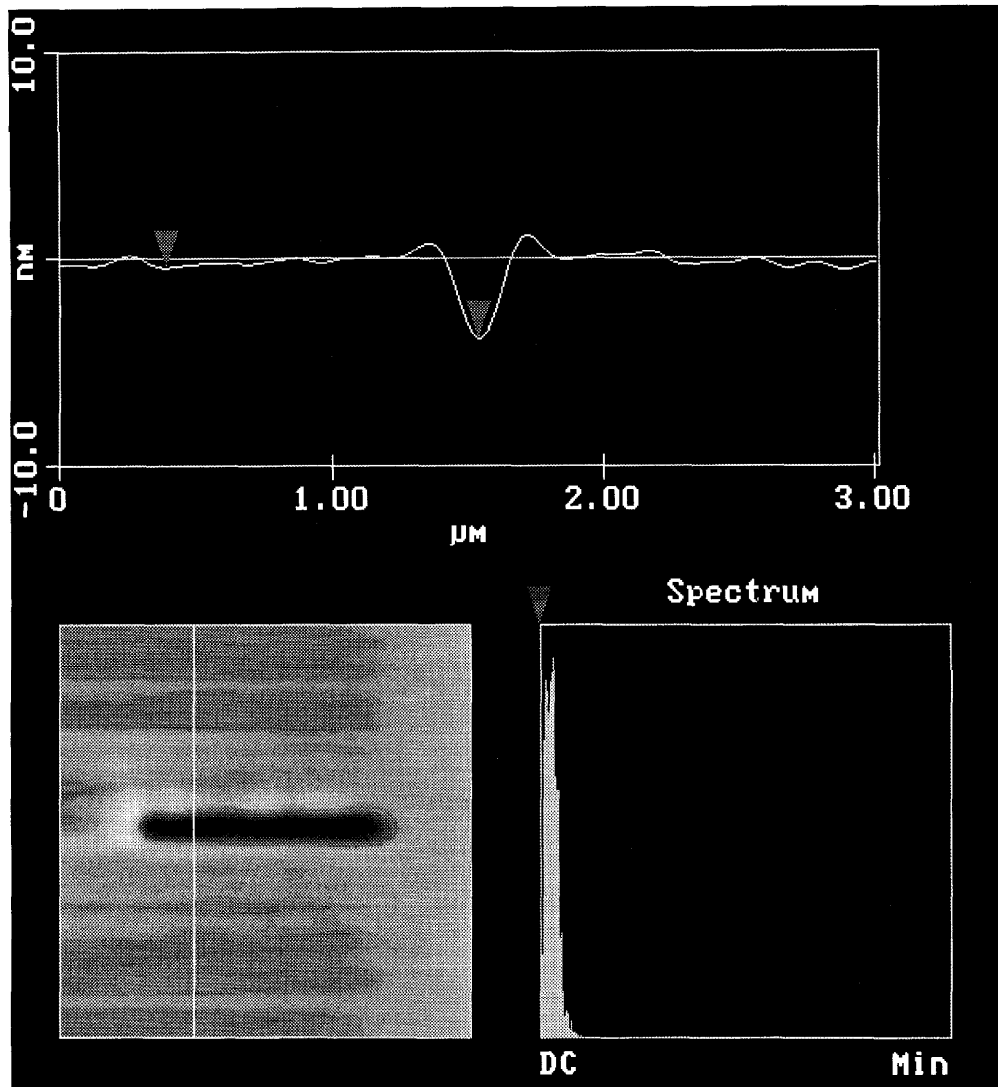


Figure 2 A surface image and section profile of a carbon film on silicon substrate

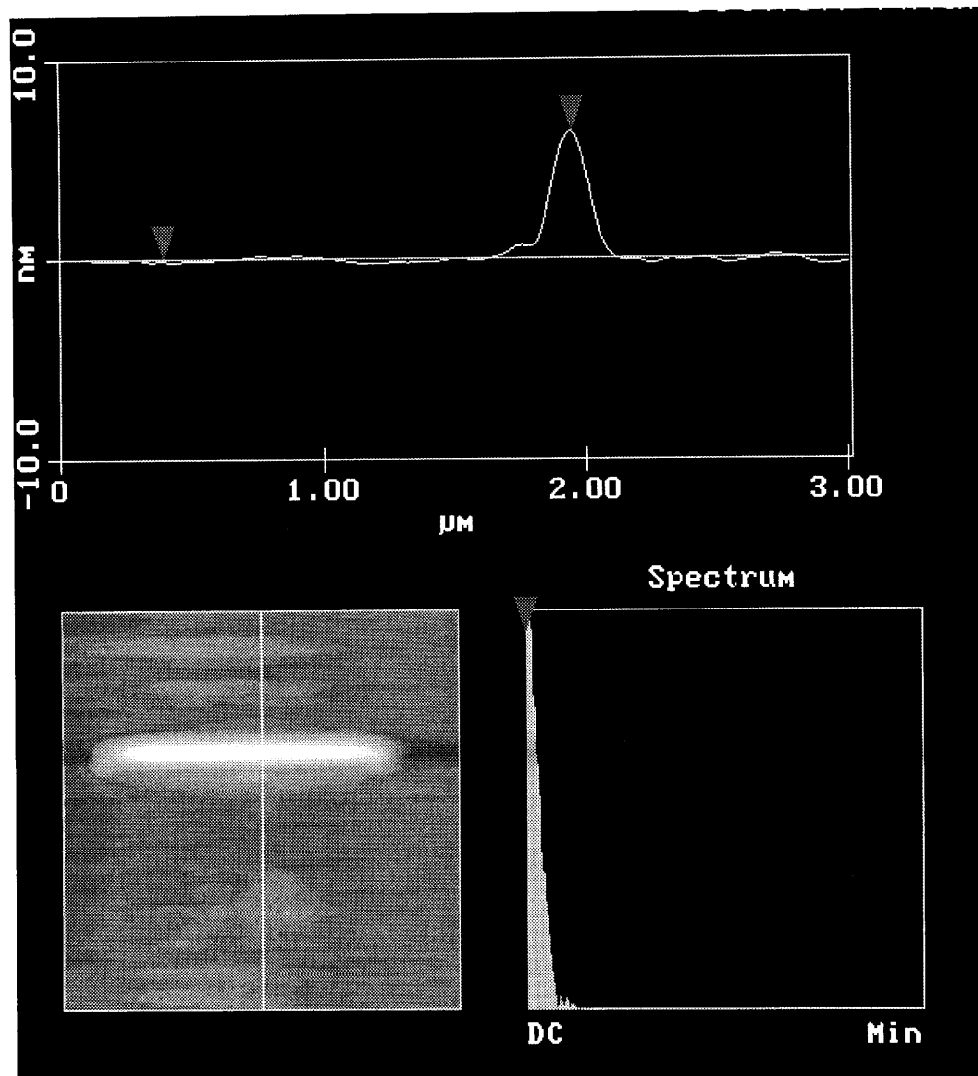


Figure 3 A surface image and section profile of a Si sample

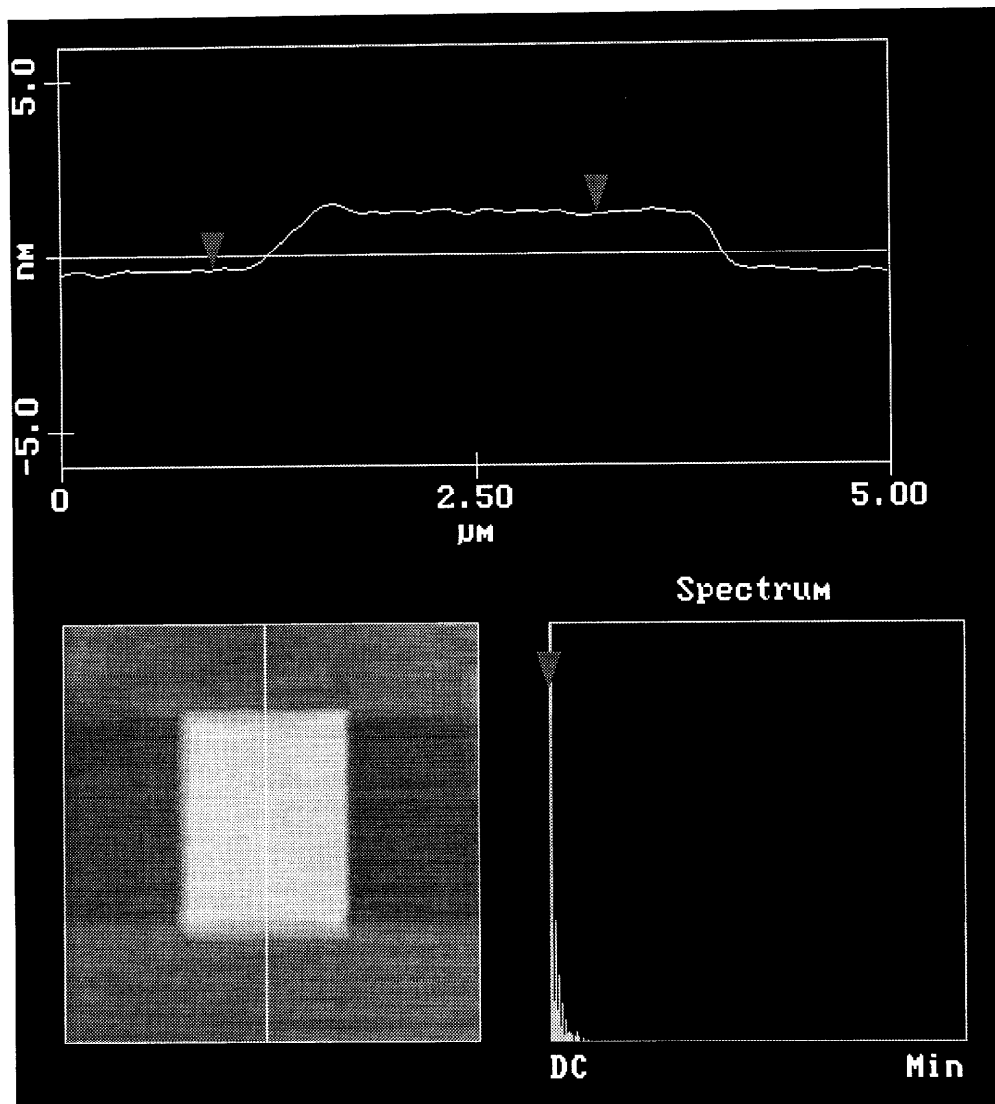


Figure 4 A surface image and section profile of a material build-up on a Si

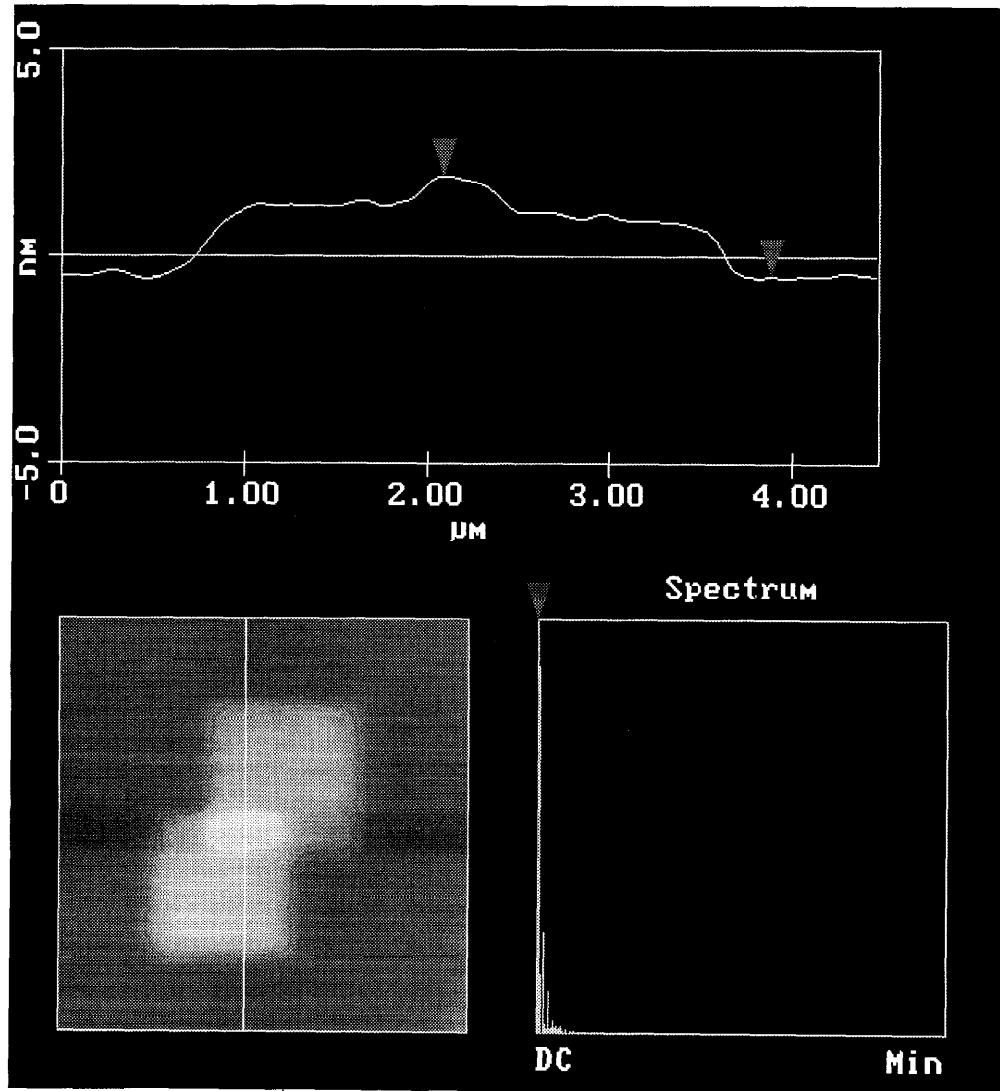


Figure 5 A surface image and section profile of two overlapped frictional material build-up patches

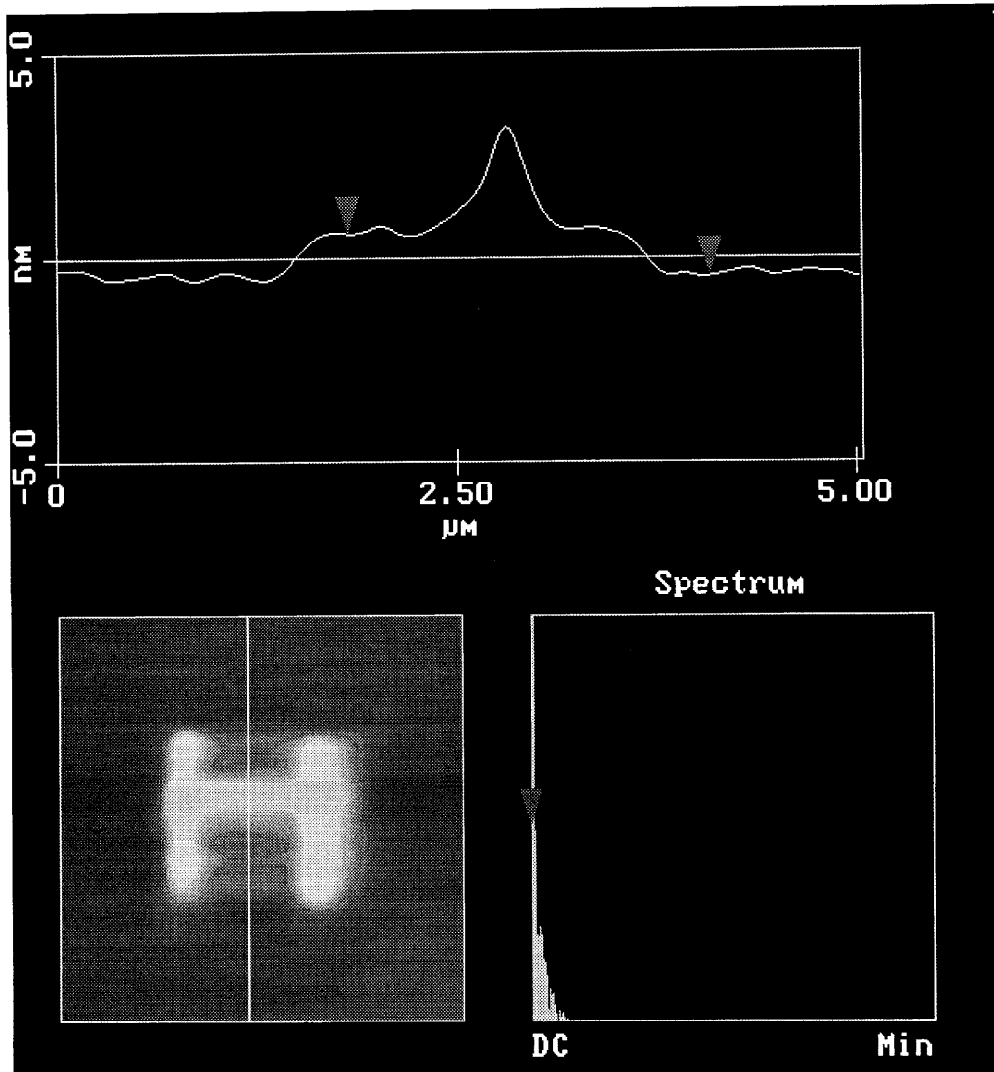


Figure 6 A surface image and section profile of a material build-up with a letter “H” shape superimposed on a frictional build-up patch

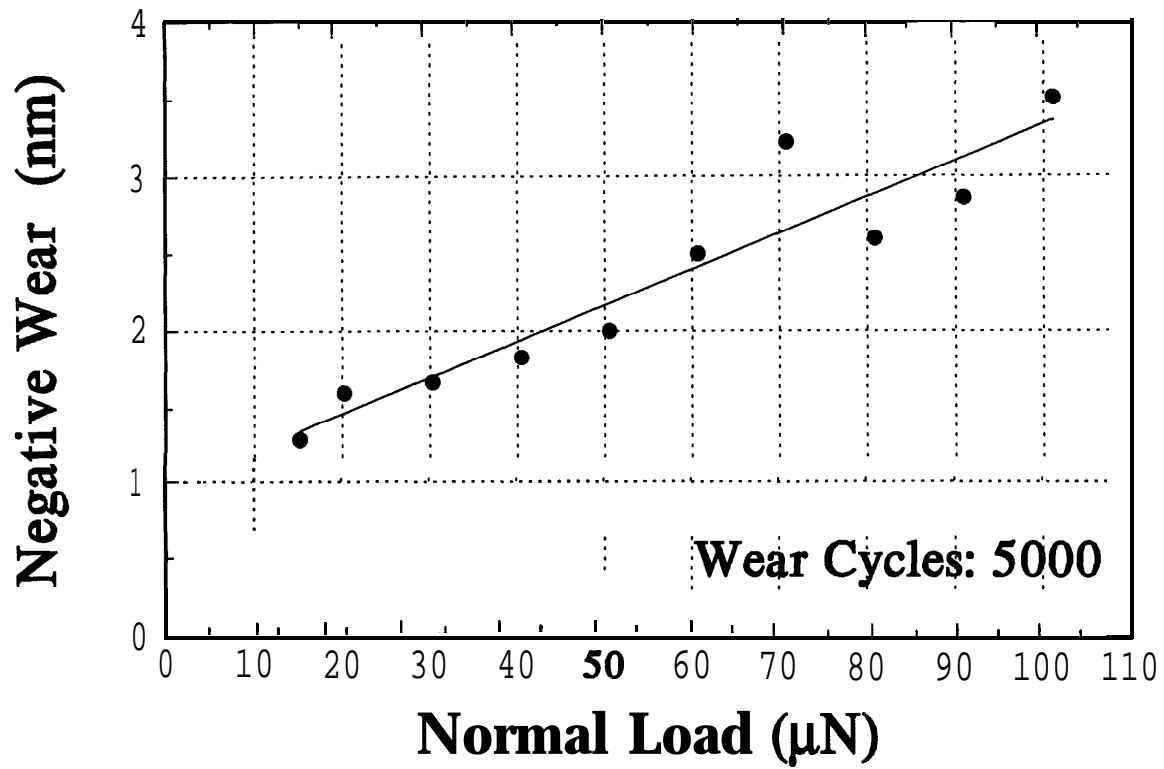


Figure 7 A plot of material build-up versus normal load

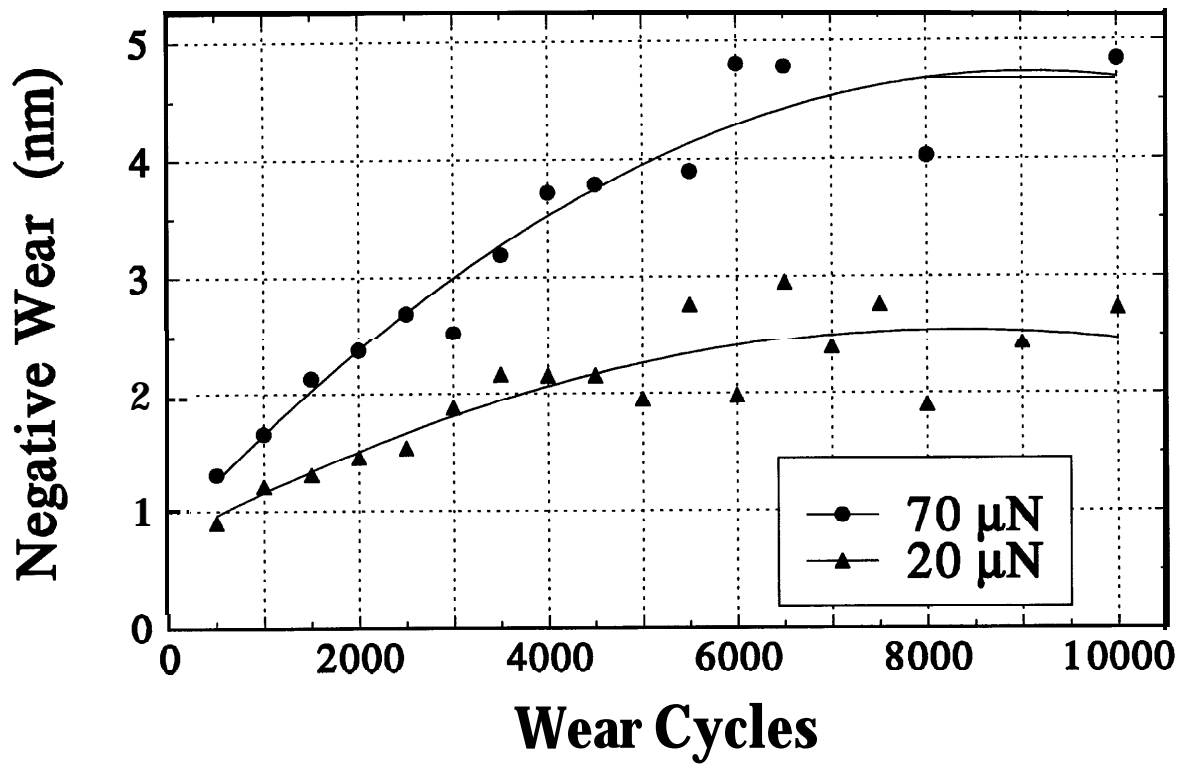


Figure 8 A plot of material build-up versus wear cycles

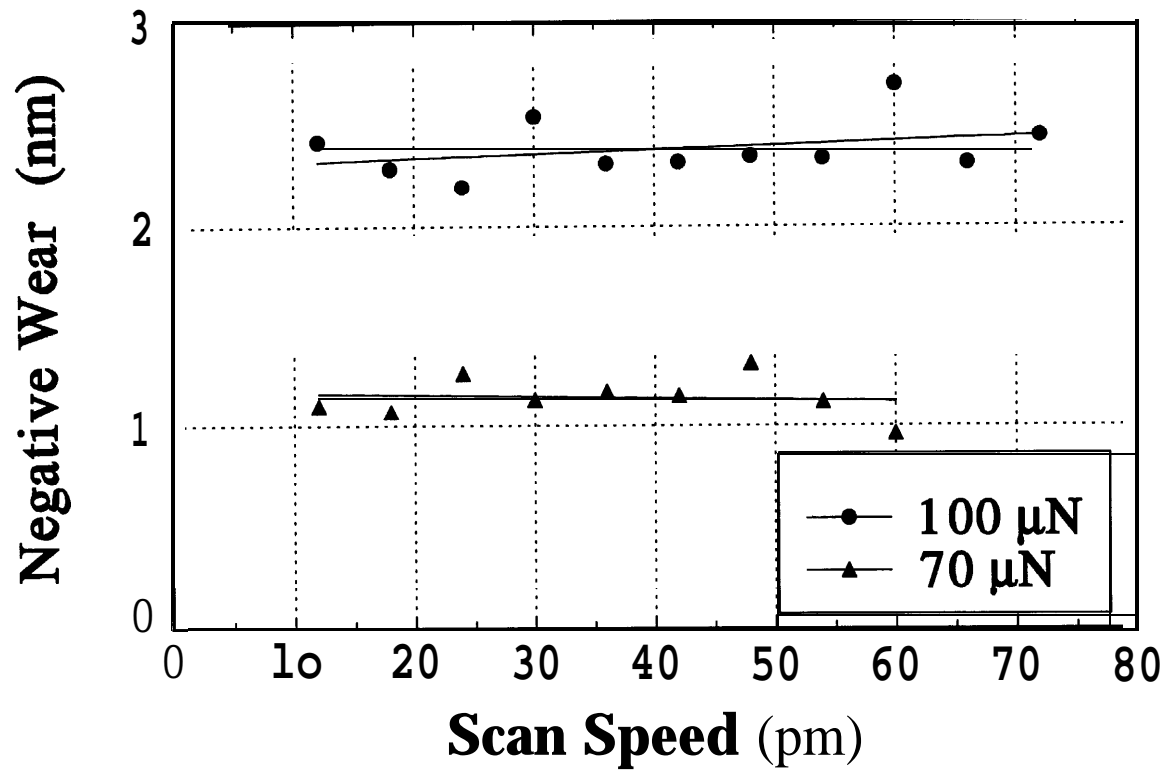


Figure 9 A plot of material build-up versus scan speed

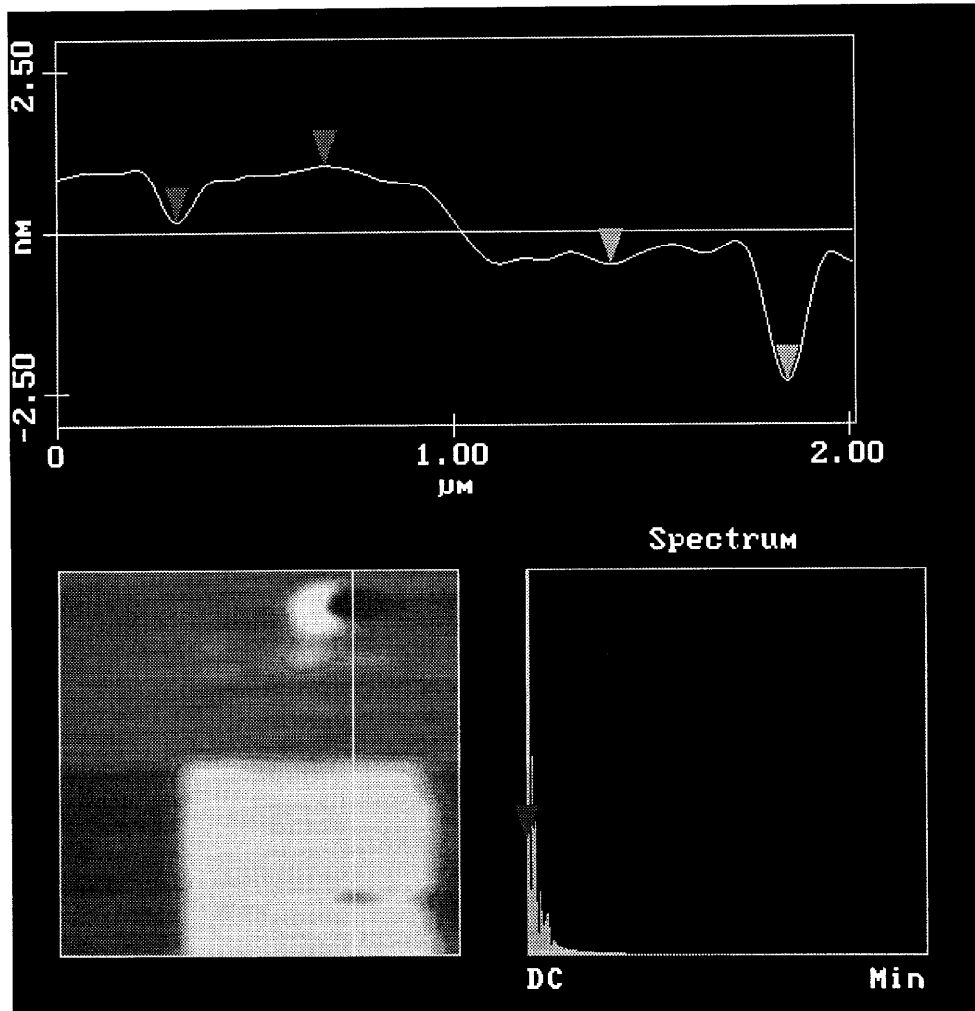


Figure 10 A surface image and section profile of the nano-indentation marks on both the build-up and the virgin surface of Si

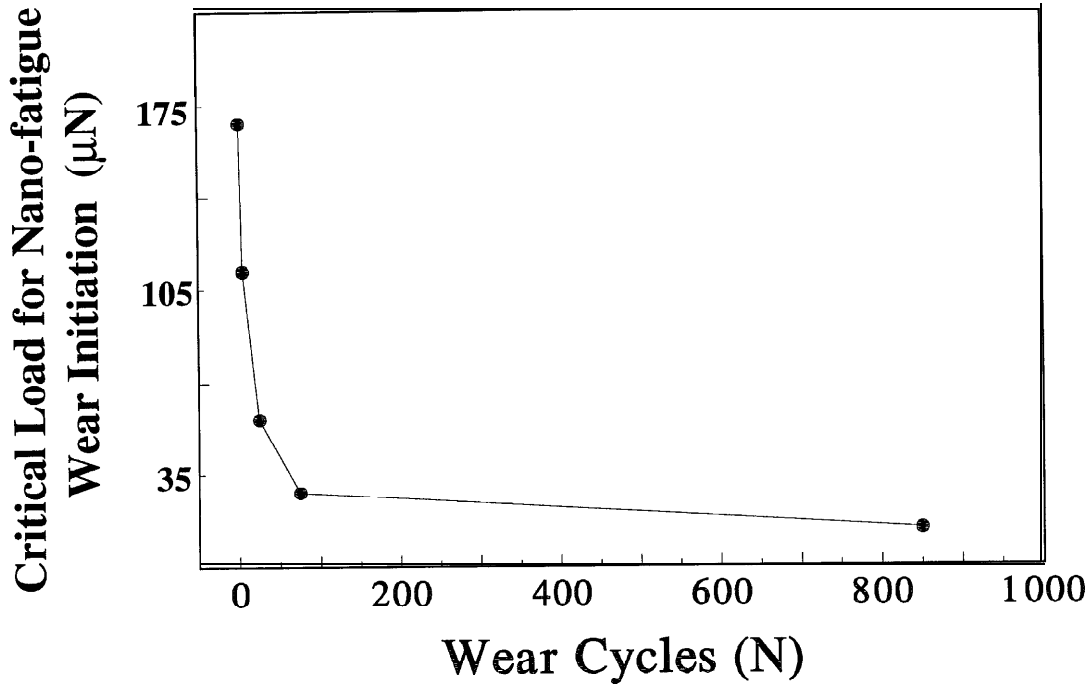


Figure 11 Critical load for nano-fatigue wear initiation versus wear cycles

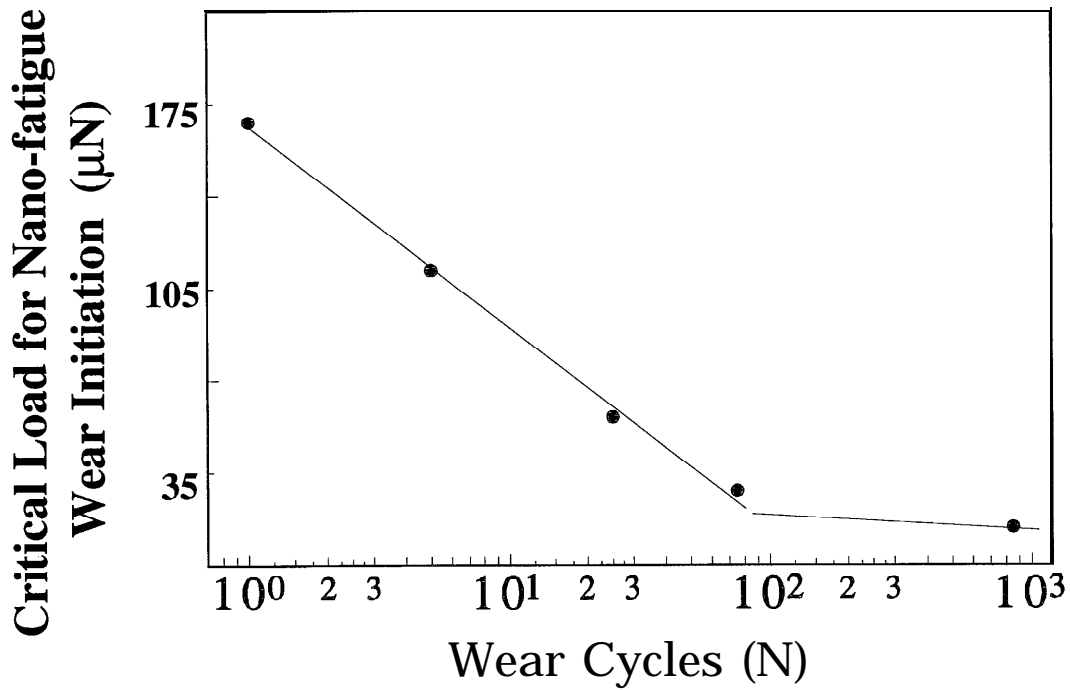


Figure 12 Critical load for nano-fatigue wear initiation versus logarithm of wear cycles

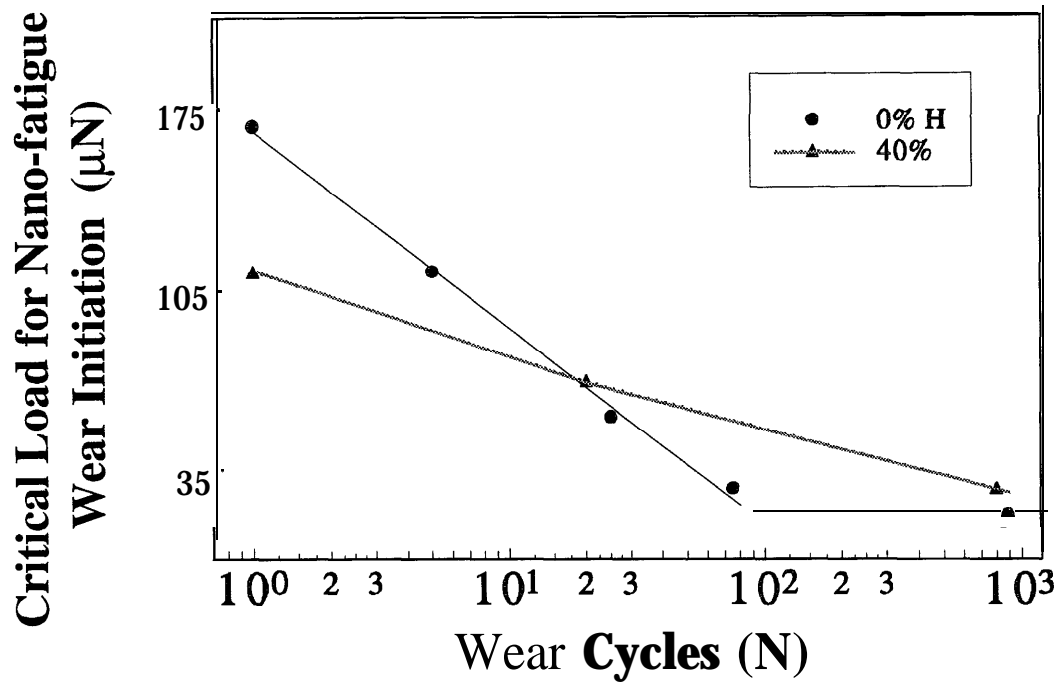


Figure 13 Curves of critical load for nano-fatigue wear initiation versus wear cycles for two carbon films

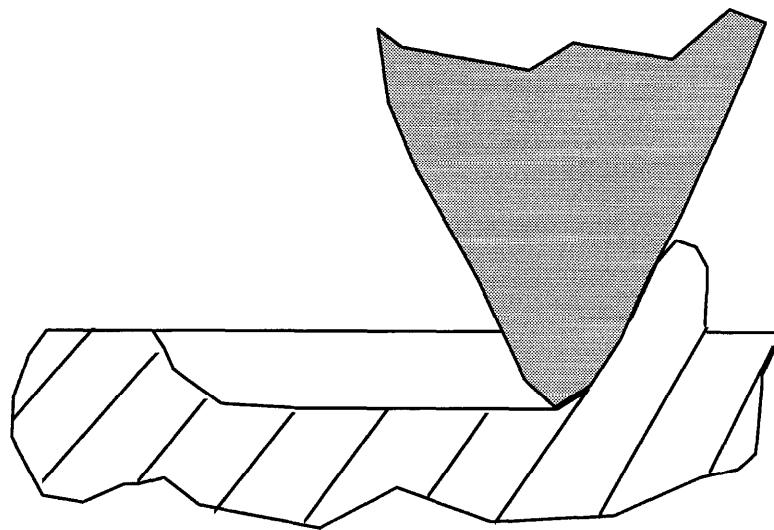


Figure 14 Plastic deformation induced by a diamond tip scratch

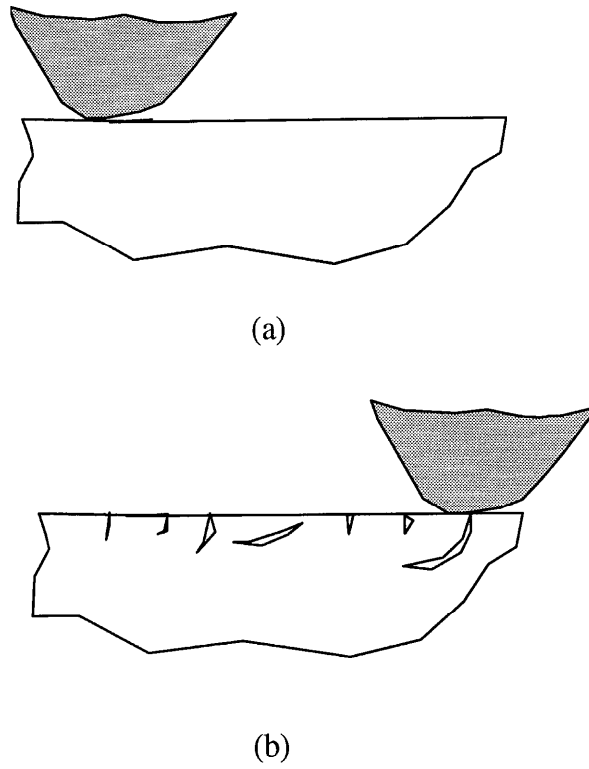


Figure 15 Cracks induced by a diamond tip scratch during a nano-fatigue wear test
(a) Before the scratch,
(b) After the scratch